


Minimal one-dimensional model of bad metal behavior from fast particle-hole scatteringYan-Qi Wang ^{1,2}, Roman Rausch,³ Christoph Karrasch,³ and Joel E. Moore^{1,2}¹*Department of Physics, University of California, Berkeley, California 94720, USA*²*Materials Sciences Division, Lawrence Berkeley National Laboratory, Berkeley, California 94720, USA*³*Institut für Mathematische Physik, Technische Universität Braunschweig, Mendelssohnstraße 3, 38106 Braunschweig, Germany*

(Received 23 March 2022; revised 20 December 2022; accepted 3 February 2023; published 10 March 2023)

A strongly interacting plasma of linearly dispersing electron and hole excitations in two spatial dimensions (2D), also known as a Dirac fluid, can be captured by relativistic hydrodynamics and shares many universal features with other quantum critical systems. We propose a one-dimensional (1D) model to capture key aspects of the 2D Dirac fluid while including lattice effects and being amenable to nonperturbative computation. When interactions are added to the Dirac-like 1D dispersion without opening a gap, we show that this kind of irrelevant interaction is able to preserve Fermi-liquid-like quasiparticle features while relaxing a zero-momentum charge current via collisions between particle-hole excitations, leading to resistivity that is linear in temperature via a mechanism previously discussed for large-diameter metallic carbon nanotubes. We further provide a microscopic lattice model and obtain numerical results via density-matrix renormalization group simulations, which support the above physical picture. The limits on such fast relaxation at strong coupling are of considerable interest because of the ubiquity of bad metals in experiments.

DOI: [10.1103/PhysRevB.107.L100301](https://doi.org/10.1103/PhysRevB.107.L100301)

Introduction. A strongly interacting plasma of linearly dispersing electron and hole excitations in two dimensions (2D), also known as a Dirac fluid, shares many universal features with other quantum critical systems. With particle-hole symmetry preserved, under an external electric field, there exists a “zero-momentum mode” in the Dirac fluid which carries a nonvanishing charge current [1–3]: Electrons and holes move symmetrically in opposite directions. Protected by conservation of momentum, in a continuous translationally invariant system, such a charge current could only be relaxed via scattering within the quasiparticles in the current. The most studied example of this kind of Dirac fluid is the electron-hole plasma in high mobility graphene at the charge neutrality point, which is believed to have Planckian-bounded dissipation [1–13], referring to a relaxation or scattering time $\tau_p \sim \hbar/k_B T$ set only by temperature and the Planck constant [14,15]. There is considerable experimental evidence for the importance of such relaxation rates as an upper bound in a broad range of “bad metals” [16–19], most famously in the linear-in-temperature resistivity of some cuprate superconductors at optimal doping, in contrast to the standard form $\rho = \rho_0 + AT^2$ of Fermi liquids. While the origin of linear-in-temperature resistivity in the normal state of high T_c superconductors at optimal doping remains an open question [14–20], hydrodynamic studies for quantum critical fluids suggest one kind of answer [1–3,11–15,21,22]: A quantum critical electron fluid with maximal Planckian dissipation is one theoretical route to linear-in- T resistivity, even if the nature of a quantum critical point near optimal doping is difficult to probe because of the intervening superconductivity.

Conceptually, if one were to take a sheet of graphene and wrap it into a metallic armchair nanotube, one might expect some signs of 2D Dirac fluid transport along the tube axis to be preserved. Indeed, Balents and Fisher argued that

interactions in a sufficiently large nanotube, while expected ultimately to open a gap, might show a linear-in- T resistivity over a range of temperatures, based on particle-hole scattering as a perturbation [23]. As nothing in the Dirac fluid picture is manifestly specific to two dimensions, one could ask whether similar features could be obtained in one spatial dimension, where metallic transport is well known to have unique features [24]. On the other hand, previous models have been studied to explore whether it is possible to relax the current in an impurity-free, nonintegrable 1D system at finite temperature, but these generally have parametrically slower relaxation than required for linear-in- T resistivity [25–28]. All these encourage us to look elsewhere for a 1D model which can support Planckian dissipation and linear-in- T resistivity, in analogy with the Dirac fluid. As more nonperturbative calculations are available in one dimension both theoretically and numerically, constructing a 1D Dirac fluid and increasing interactions to strong coupling is a test of one origin of Planckian dissipation.

In this Letter, we propose a 1D model with no observable gap, and use a kinetic theory approach to determine its resistivity [29–34]. To check that this physics can be realized in a solid, we then introduce a microscopic lattice model that manifests the aforementioned internal scattering process. We further use time-dependent density-matrix renormalization-group (DMRG) simulations [35–38] to confirm the gaplessness of the lattice model, and compute the current relaxation at finite temperature.

Continuous model. The low-energy theory of a noninteracting 1D metal can be obtained by linearizing the spectrum near the Fermi level. When the Fermi points for the left- and right-moving linear branches coincide with each other, we arrive at a Dirac-like crossing, as shown in Fig. 1(a). The linearized free Hamiltonian around the Fermi point, H_0 , can

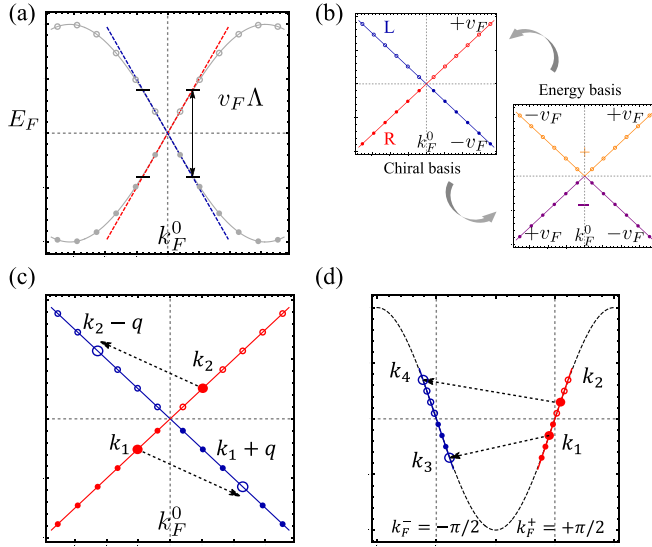


FIG. 1. Fermionic spectrum linearization and scattering processes based on it. (a) A 1D noninteracting metallic band can be linearized close to the Fermi level E_F within the energy cutoff $v_F \Lambda$. Note that the left Fermi point and right Fermi point coincide at k_F^0 . (b) The linearized spectrum can be described by the chiral basis, with the red modes moving to the right with velocity $+v_F$ and blue modes moving to the left with velocity $-v_F$ in real space. The linearized spectrum can also be written in the energy basis, where states are labeled by positive (orange) and negative (purple) energies. The velocities for different quasiparticles are also shown in the figure. (c) Illustration for particle-hole scattering or fast umklaplike scattering (FUS). Two right movers with momentum k_1 and k_2 are scattered to the left-moving branch with momentum $k_1 + q$ and $k_2 - q$. Note that the total momentum is conserved in this process. (d) Conventional umklapp scattering in 1D metal for two right movers (k_1, k_2) scattering into two left movers (k_3, k_4). Note that for conventional umklapp scattering, the Fermi points for the right and left movers are different (say at $k_F^\pm = \pm\pi/2$). The momentum is conserved only up to a reciprocal vector $G = 2\pi$, i.e., there is a large momentum transfer in the scattering process.

be written in a chiral basis as

$$H_0 = v_F \int \frac{dk}{2\pi} k [\psi_R^\dagger(k) \psi_R(k) - \psi_L^\dagger(k) \psi_L(k)], \quad (1)$$

where $\psi_R(k)$ and $\psi_L(k)$ stand for the annihilation operators for right- and left-moving chiral fermion modes at one-dimensional momentum k , respectively, and v_F is the Fermi velocity near the Fermi level. The above chiral basis can be transformed into the energy basis [12,31], in which $\gamma_+(k)$ and $\gamma_-(k)$ annihilate an electron with energy above and below the Dirac node, respectively,

$$\begin{pmatrix} \gamma_+(k) \\ \gamma_-(k) \end{pmatrix} = \frac{1}{2} \begin{pmatrix} 1 + \vartheta(k) & 1 - \vartheta(k) \\ 1 - \vartheta(k) & 1 + \vartheta(k) \end{pmatrix} \begin{pmatrix} \psi_R(k) \\ \psi_L(k) \end{pmatrix}, \quad (2)$$

where $\vartheta(x) = 1$ for $x > 0$ and $\vartheta(x) = -1$ for $x < 0$. Note that the density of states vanishes at the Dirac node, so hereafter we can neglect the singularity at $k = 0$ itself. With this, the free Hamiltonian is transformed into the following form:

$$H_0 = v_F \int \frac{dk}{2\pi} k [\gamma_+^\dagger(k) \gamma_+(k) - \gamma_-^\dagger(k) \gamma_-(k)]. \quad (3)$$

Both chiral and energy bases are plotted in Fig. 1(b).

Now we study the full Hamiltonian H with an interaction H_{int} turned on:

$$H = H_0 + H_{\text{int}}. \quad (4)$$

We would like the interaction to introduce the following fast umklaplike scattering (FUS) among the chiral fermions [39]:

$$H_{\text{int}} = \int \frac{dk_1}{2\pi} \frac{dk_2}{2\pi} \frac{dq}{2\pi} V(q) [\psi_R^\dagger(k_1 + q) \psi_R^\dagger(k_2 - q) \psi_L(k_2) \times \psi_L(k_1) + \psi_L^\dagger(k_1 + q) \psi_L^\dagger(k_2 - q) \psi_R(k_2) \psi_R(k_1)]. \quad (5)$$

This process takes two electrons on the same branch to the opposite branch, as shown in Fig. 1(c) [40–43]. Unlike the conventional umklapp scattering for a one-component model [see Fig. 1(d)], the FUS defined here does not carry large momentum transfer, as the left- and right-moving branches' Fermi points coincide at the Dirac node. One can alternately view one of the processes as the scattering of a hole rather than an electron. We will see in a particle-hole symmetric system, a current of oppositely directed particles and holes can have zero total momentum, allowing the current to relax through momentum-conserving collisions.

The interaction Eq. (5) can also be written in the energy basis

$$H_{\text{int}} = \sum_{\lambda_1 \lambda_2 \lambda_3 \lambda_4} \int \frac{dk_1}{2\pi} \frac{dk_2}{2\pi} \frac{dq}{2\pi} T_{\lambda_1 \lambda_2 \lambda_3 \lambda_4}(k_1, k_2, q) \times \gamma_{\lambda_4}^\dagger(k_1 + q) \gamma_{\lambda_3}^\dagger(k_2 - q) \gamma_{\lambda_2}(k_2) \gamma_{\lambda_1}(k_1), \quad (6)$$

where the $\lambda_{1, \dots, 4}$ in the summation take the value of \pm and the structure factor $T_{\lambda_1 \lambda_2 \lambda_3 \lambda_4}(k_1, k_2, q) = T_{\lambda_1 \lambda_2 \lambda_3 \lambda_4}^2 + T_{\lambda_1 \lambda_2 \lambda_3 \lambda_4}^3$ where $T_{\lambda_1 \lambda_2 \lambda_3 \lambda_4}^2 = V(q) [\lambda_1 \vartheta(k_1) - \lambda_4 \vartheta(k_1 + q)] [\lambda_2 \vartheta(k_2) - \lambda_3 \vartheta(k_2 - q)] / 16$ and $T_{\lambda_1 \lambda_2 \lambda_3 \lambda_4}^3 = V(q) [1 - \lambda_1 \lambda_3 \vartheta(k_1^2 + qk_1)] [1 - \lambda_2 \lambda_3 \vartheta(k_2^2 - qk_2)] / 16$ are the matrices which indicate the scattering amplitudes among electrons with positive and negative energy.

Kinetic theory. One can use the kinetic (hydrodynamic) theory to describe transport properties [29–33]. Note that, for the particle density $\rho(x) = \psi_R^\dagger(x) \psi_R(x) + \psi_L^\dagger(x) \psi_L(x)$, the continuity equation $\partial_t \rho(x) + \partial_x j(x) = 0$ gives the $U(1)$ current density $j(x) = v_F [\psi_R^\dagger(x) \psi_R(x) - \psi_L^\dagger(x) \psi_L(x)]$. Assuming the charge carried by each particle (hole) is $+Q$ ($-Q$), the total charge current J reads [12,31]

$$J = v_F Q \sum_{r=R,L} \int \frac{dk}{2\pi} r \psi_r^\dagger(k) \psi_r(k) \quad (7a)$$

$$= v_F Q \sum_{\lambda=\pm} \int \frac{dk}{2\pi} \frac{\lambda k}{|k|} \gamma_\lambda^\dagger(k) \gamma_\lambda(k). \quad (7b)$$

Note that in Eq. (7a), we have $r = 1$ for right movers (R) and $r = -1$ for left movers (L). Similarly, the total momentum reads

$$P = \sum_{r=R,L} \int \frac{dk}{2\pi} k \psi_r^\dagger(k) \psi_r(k) = \sum_{\lambda} \int \frac{dk}{2\pi} k \gamma_\lambda^\dagger(k) \gamma_\lambda(k). \quad (8)$$

We define the distribution functions under the energy basis γ_{\pm} at time t as

$$f_{\lambda}(k, t) = \langle \gamma_{\lambda}^{\dagger}(k, t) \gamma_{\lambda}(k, t) \rangle. \quad (9)$$

In the equilibrium, without external perturbation, these are related to the Fermi distribution function $f^0(p)$, such that $f_{\pm}(k, t) = f^0(\pm\epsilon_k) = [e^{(\pm\epsilon_k - \mu)/k_B T} + 1]^{-1}$ with μ the chemical potential. From standard bosonization [44], one can safely assume that turning on the interaction will neither open a gap, nor have an immediate modification of the single-particle spectrum of Eq. (3). Then the Fermi-liquid picture survives, $\epsilon_{\lambda}(k) = \lambda v_F |k|$, with $\lambda = \pm$ for two flavors of quasiparticles: the positive energy ones with the distribution function $f_{+}(k, t)$, and the negative energy ones with the distribution function $f_{-}(k, t)$.

The quantum Boltzmann equation with collisions reads [12,31,45]

$$\left[\frac{\partial}{\partial t} + QE(t) \frac{\partial}{\partial k} \right] f_{\lambda}(k, t) = -\frac{2\pi}{v_F} \int \frac{dk_1}{2\pi} \frac{dq}{2\pi} \mathcal{R}. \quad (10)$$

The integrand $\mathcal{R} = \mathcal{R}_1 + \mathcal{R}_2$ [46], capturing the scattering among excitations, can be derived by a simple application of Fermi's golden rule together with the interaction in Eq. (6). The first part is the scattering among different flavors of excitations (particle-hole to particle-hole) $\mathcal{R}_1 = \delta[(|k| - |k_1|) - (|k + q| - |k_1 - q|)] R_1(k, k_1, q) \{ f_{\lambda}(k, t) f_{-\lambda}(k_1, t) [1 - f_{\lambda}(k + q, t)] [1 - f_{-\lambda}(k_1 - q, t)] - [1 - f_{\lambda}(k, t)] [1 - f_{-\lambda}(k_1, t)] f_{\lambda}(k + q, t) f_{-\lambda}(k_1 - q, t) \}$, with scattering amplitude $R_1(k, k_1, q) = 4|T_{+--+}(k, k_1, q) - T_{-+-}(k, k_1, -k - q + k_1)|^2$. The second part \mathcal{R}_2 captures the scattering among the same flavors of excitations (particles to particles or holes to holes), which will not contribute to the resistivity at leading order [47]. To solve Eq. (10), we first parametrize the change in f_{λ} from its equilibrium value by using the ansatz [12,45]

$$f_{\lambda}(k, \omega) = 2\pi \delta(\omega) f^0(\lambda\epsilon_k) + Q \frac{kE(\omega)}{|k|} f^0(\lambda\epsilon_k) \times [1 - f^0(\lambda\epsilon_k)] g_{\lambda}(\epsilon_k, \omega), \quad (11)$$

with $g_{\lambda}(\epsilon_k, \omega)$ a function to be determined, and we have replaced $f_{\lambda}(k, t)$ with its Fourier counterpart in the frequency domain $f_{\lambda}(k, \omega)$. When $\mu = 0$, the system is at the particle-hole symmetric point, and an applied electric field $E(\omega)$ generates deviations in the distribution functions for particles and holes with opposite signs. This is due to the fact that the driving term Eq. (10) is odd under $\lambda \rightarrow -\lambda$, thus the deviation also has to be asymmetric in λ : $g_{\lambda}(\epsilon_k, \omega) = \lambda g(k, \omega)$. In coordinate space, there will be newly generated holes (particles) moving in alignment (antialignment) with the external electric field. This can be viewed as the generation of particle-hole pairs. For the states within the orange and purple squares shown in Fig. 2(a), at the same k point, the particle and hole have opposite momentum, and each particle-hole pair has zero total momentum defined by Eq. (8) in the presence of particle-hole symmetry. On the other hand, since the particles and holes carry opposite charge, if they move in opposite directions, the total current given by Eq. (7) is nonzero. Substituting Eq. (11) into Eq. (10), one could derive a solution for g via the variational methods [12,44,45]. Combined with Eq. (7b), with the definition of charge conductivity $\sigma = J/E$,

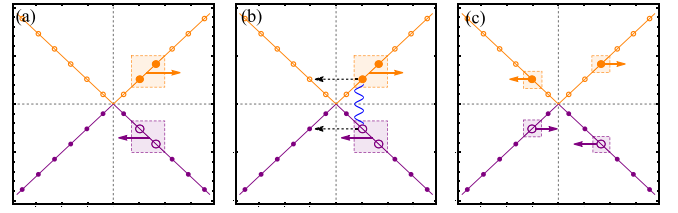


FIG. 2. Generation and relaxation of charge current in a particle-hole symmetric system. (a) Generation of the zero-momentum mode under an external electric field. The net charge current for the states in the plot is $J = 4Qv_F$. (b) Collision between the particle and hole via the interaction (wavy line) based on the initial state shown in (a). (c) Final state after the scattering process in (b), which has zero momentum and zero charge current.

we arrive at

$$\sigma(\omega) = \frac{\langle J \rangle}{E(\omega)} \approx \frac{2Q^2}{h} \frac{\hbar v_F}{-i\hbar\omega + \kappa k_B T}, \quad (12)$$

where κ is associated with interflavor scattering,

$$\kappa = \int \frac{d\tilde{k}}{2\pi} \frac{d\tilde{q}}{2\pi} \frac{4R_1(\tilde{k}, -\tilde{k}, \tilde{q})v_F^2}{(e^{-|\tilde{k}|} + 1)(e^{|\tilde{k}|} + 1)(e^{|\tilde{k} + \tilde{q}|} + 1)(e^{-|\tilde{k} + \tilde{q}|} + 1)}. \quad (13)$$

As a check for the validity of our kinetic theory, we first notice that in the collisionless limit $\mathcal{R} = \mathcal{R}_1 = \mathcal{R}_2 = 0$ such that $\kappa = 0$, we shall see

$$\sigma(\omega) \approx \frac{2Q^2}{h} \frac{\hbar v_F}{-i\hbar\omega + \eta}, \quad (14)$$

with η a positive infinitesimal. This is consistent with the bosonization results for a clean system in 1D [48]. The presence of a Drude peak in the low-frequency limit is the signature of ballistic transport [48,49].

In the presence of FUS, $\kappa \neq 0$. Compared with the low-frequency diverging result for the collisionless case in Eq. (14), the conductivity with collisions has some broadening at finite temperature. This shows that the zero-momentum mode can be relaxed solely by the momentum-conserved internal scattering process among excitations. Such a physical picture is plotted in Figs. 2(b) and 2(c). From Eq. (12), we find the resistivity $\rho = 1/\sigma$ in the dc limit has a linear-in- T dependence, i.e., the Planckian dissipation

$$\rho(\omega \rightarrow 0) \sim AT, \quad (15)$$

with the coefficient $A = \pi\kappa k_B/Q^2 v_F$. A one-dimensional Dirac system whose linear dispersion survives the interaction can be captured by a single model-dependent parameter, the Fermi velocity v_F . Combined with the temperature T , the only timescale in the continuous limit is the Planckian time $\tau_p = \hbar/k_B T$. Such a timescale gives the scattering rate for particle-hole excitations in an impurity-free Dirac system, and sets up an upper bound for the resistivity at finite temperature $\rho = AT$. The coefficient $A \propto |V(q)/v_F|^2$, which shows that the resistivity is also positively related to the interaction strength in the perturbative region, in accordance with the previous results in wrapping a graphene sheet to large-diameter metallic carbon nanotubes [23].

Lattice model. We start from a fermionic lattice model which possesses a low-energy Hamiltonian Eq. (4) that reads

$$\begin{aligned}\tilde{H} &= \tilde{H}_0 + \tilde{H}_2 + \tilde{H}_3, \\ \tilde{H}_0 &= +t \sum_i [-i\xi a_i^\dagger b_i + i\xi b_i^\dagger a_i - ib_i^\dagger a_{i+1} + ia_{i+1}^\dagger b_i], \\ \tilde{H}_2 &= \frac{V_2}{4} \sum_i [(a_i^\dagger b_i - b_i^\dagger a_i)(a_{i+1}^\dagger b_{i+1} - b_{i+1}^\dagger a_{i+1}) \\ &\quad + (b_i^\dagger a_{i+1} - a_{i+1}^\dagger b_i)(b_{i+1}^\dagger a_{i+2} - a_{i+2}^\dagger b_{i+1})], \\ \tilde{H}_3 &= \frac{V_3}{4} \sum_i [(a_i^\dagger a_i - b_i^\dagger b_i)(a_{i+1}^\dagger a_{i+1} - b_{i+1}^\dagger b_{i+1}) \\ &\quad + (b_i^\dagger b_i - a_{i+1}^\dagger a_{i+1})(b_{i+1}^\dagger b_{i+1} - a_{i+2}^\dagger a_{i+2})].\end{aligned}\quad (16)$$

Here, the \tilde{H}_0 stands for the free Hamiltonian and $\tilde{H}_2 + \tilde{H}_3$ is the interaction. The kinetic part \tilde{H}_0 can be connected to the integrable XX model [50]. The addition of $\tilde{H}_2 + \tilde{H}_3$ breaks the integrability (see a plot of the crossover of level statistics from Poisson to Wigner-Dyson in the Supplemental Material [44,51]), which justifies the legitimacy of using kinetic equations in our analytic calculations. The form of the interaction is obtained by seeking to construct a Hamiltonian which has FUS as its naive continuum limit, then symmetrizing the Hamiltonian, i.e., ensuring that it does not include a relevant, gap-opening dimerization at least at leading order. The a_i^\dagger and b_i^\dagger denote the creation operators for two distinct degrees of freedom at the same point in the i th unit cell. When $\xi = 1$, the Bloch Hamiltonian for \tilde{H}_0 can be linearized around $k = 0$, and has a Dirac-like structure as given in Eq. (1). When $V_2 = V_3$, to the leading order the interaction will only contain the FUS given in Eq. (5). We further provide the charge current density operator $j_{i+1} = (+tQ)[b_i^\dagger a_{i+1} + a_{i+1}^\dagger b_i]$ which with density-density interactions satisfies the standard continuity equation $\partial \rho_i(t)/\partial t + (j_{i+1} - j_i) = 0$ for the local charge density of each unit cell $\rho_n = Q(a_n^\dagger a_n + b_n^\dagger b_n)$ [44]. The dc conductivity may be found via the Kubo formula

$$\sigma = \lim_{T \rightarrow \infty} \lim_{N \rightarrow \infty} \frac{1}{NT} \text{Re} \int_0^{t_M} dt \langle J(t)J(0) \rangle, \quad (17)$$

where the total charge current for a system with N unit cells at time t is $J(t) = \sum_{i=1}^N j_i(t)$ [28,52–55].

DMRG results. We first confirm that the lattice model Eq. (16) is gapless for $V_2, V_3 < 4t$ using the density-matrix renormalization group [35,44]. To evaluate the conductivity, we proceed using standard techniques [56–58]: Finite temperatures are implemented by going from a pure state to the density operator. We enlarge the local Hilbert space to include an auxiliary part, which is traced out when performing expectation values. The state at $\beta = 1/T = 0$ is exactly initialized on a finite chain with $L = 96$ and then propagated to the desired β . After that, the state is perturbed by applying the current operator and propagated in real time up, which yields the current correlation function $\langle J(t)J \rangle/L$. We have chosen a system size that is large enough so as not to allow the current to reach the finite system boundaries at the end of the simulation. Since the Hamiltonian contains more than nearest-neighbor interactions, we cannot use a standard time-

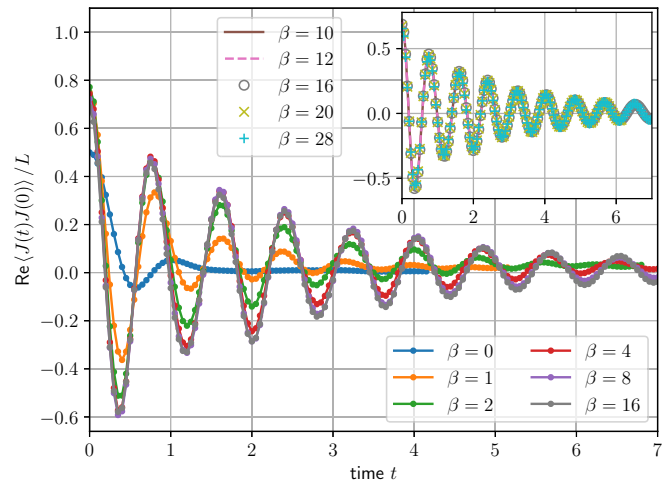


FIG. 3. Time-dependent current-current correlation function at $V_2 = V_3 = 3$ calculated using DMRG.

evolving block decimation algorithm but instead employ the time-dependent variational principle (TDVP) [59]. We use the two-site TDVP algorithm [44,59–61].

For small $V = V_2 = V_3$, the entanglement buildup is relatively small, but we are also very close to the integrable point $V = 0$, resulting in very long relaxation times, and vice versa for large V . Faced with these trade-offs, we find that we need to go to $V = 3$ to be able to evaluate the current correlations. The results are shown in Fig. 3. It turns out that we still cannot reach timescales which are long enough to quantitatively compute the integral in Eq. (17), and we observe that below $T = 1/8$ – $1/10$, the different curves essentially collapse onto one curve for the times we are able to access. Assuming that this collapse will continue to hold for the inaccessible times as well, this means that the integral over $\langle J(t)J \rangle/L$ becomes independent of T in this regime. Due to the prefactor of $1/T$ in Eq. (17), this points towards a resistivity which is indeed proportional to T in the low-temperature regime. The seemingly complicated model Eq. (16) provides a route to realize the conjectured Planckian upper bound to the resistivity for a class of realistic interacting semimetals in 1D with local and nonrandom interactions [23,62].

Conclusion. We proposed a model for a 1D Dirac fermionic system as well as its lattice counterpart, and showed that quasiparticles broaden from collisions at finite temperature compared with the well-known diverging results for 1D two-channel ballistic transport. Verifying transport similar to that proposed for the 2D Dirac liquid in a 1D model provides an alternative point of view on the origin of bad metallic behavior, and observing the dominance of umklapp-like scattering in our model complements other possibilities for transport theory in one dimension dominated by other irrelevant operators [63]. The analytical and numerical methods available to explore transport in low spatial dimensions make it feasible to search for evidence of other physics originally proposed for higher dimensions, as we have done here for the Dirac fluid [64–68].

Acknowledgments. This work was supported as part of the Center for Novel Pathways to Quantum Coherence in Materials, an Energy Frontier Research Center funded by the

U.S. Department of Energy, Office of Science, Basic Energy Sciences (Y.-Q.W. and J.E.M.). R.R. and C.K. acknowledge support by the Deutsche Forschungsgemeinschaft (DFG, German Research Foundation) through the Emmy Noether

program (KA3360/2-1). Y.-Q.W. thanks Vir Bulchandani and Jyong-Hao Chen for the early introductions to transport theory. J.E.M. acknowledges support from a Simons Investigatorship and thanks Chandra Varma for helpful discussions.

-
- [1] S. A. Hartnoll, P. K. Kovtun, M. Müller, and S. Sachdev, Theory of the Nernst effect near quantum phase transitions in condensed matter and in dyonic black holes, *Phys. Rev. B* **76**, 144502 (2007).
- [2] M. Müller and S. Sachdev, Collective cyclotron motion of the relativistic plasma in graphene, *Phys. Rev. B* **78**, 115419 (2008).
- [3] M. Müller, L. Fritz, and S. Sachdev, Quantum-critical relativistic magnetotransport in graphene, *Phys. Rev. B* **78**, 115406 (2008).
- [4] J. Crossno, J. K. Shi, K. Wang, X. Liu, A. Harzheim, A. Lucas, S. Sachdev, P. Kim, T. Taniguchi, K. Watanabe, T. A. Ohki, and K. C. Fong, Observation of the Dirac fluid and the breakdown of the Wiedemann-Franz law in graphene, *Science* **351**, 1058 (2016).
- [5] A. Lucas, Sound waves and resonances in electron-hole plasma, *Phys. Rev. B* **93**, 245153 (2016).
- [6] A. Lucas, J. Crossno, K. C. Fong, P. Kim, and S. Sachdev, Transport in inhomogeneous quantum critical fluids and in the Dirac fluid in graphene, *Phys. Rev. B* **93**, 075426 (2016).
- [7] T. V. Phan, J. C. W. Song, and L. S. Levitov, Ballistic heat transfer and energy waves in an electron system, [arXiv:1306.4972](https://arxiv.org/abs/1306.4972).
- [8] Z. Sun, D. N. Basov, and M. M. Fogler, Adiabatic Amplification of Plasmons and Demons in 2D Systems, *Phys. Rev. Lett.* **117**, 076805 (2016).
- [9] Z. Sun, D. N. Basov, and M. M. Fogler, Universal linear and nonlinear electrodynamics of a Dirac fluid, *Proc. Natl. Acad. Sci. USA* **115**, 3285 (2018).
- [10] A. Lucas and K. C. Fong, Hydrodynamics of electrons in graphene, *J. Phys.: Condens. Matter* **30**, 053001 (2018).
- [11] P. Gallagher, C. S. Yang, T. Lyu, F. Tian, R. Kou, H. Zhang, K. Watanabe, T. Taniguchi, and F. Wang, Quantum-critical conductivity of the Dirac fluid in graphene, *Science* **364**, 158 (2019).
- [12] L. Fritz, J. Schmalian, M. Müller, and S. Sachdev, Quantum critical transport in clean graphene, *Phys. Rev. B* **78**, 085416 (2008).
- [13] Mark J. H. Ku, T. X. Zhou, Q. Li, Y. J. Shin, J. K. Shi, C. Burch, L. E. Anderson, A. T. Pierce, Y. Xie, A. Hamo, U. Vool, H. Zhang, F. Casola, T. Taniguchi, K. Watanabe, M. M. Fogler, P. Kim, A. Yacoby, and R. L. Walsworth, Imaging viscous flow of the Dirac fluid in graphene, *Nature (London)* **583**, 537 (2020).
- [14] J. Zaanen, Why the temperature is high, *Nature (London)* **430**, 512 (2004).
- [15] J. Zaanen, Planckian dissipation, minimal viscosity and the transport in cuprate strange metals, *SciPost Phys.* **6**, 061 (2019).
- [16] J. Orenstein, G. A. Thomas, A. J. Millis, S. L. Cooper, D. H. Rapkine, T. Timusk, L. F. Schneemeyer, and J. V. Wazczak, Frequency- and temperature-dependent conductivity in $\text{YBa}_2\text{Cu}_3\text{O}_{6+x}$ crystals, *Phys. Rev. B* **42**, 6342 (1990).
- [17] J. A. N. Bruin, H. Sakai, R. S. Perry, and A. P. Mackenzie, Similarity of scattering rates in metals showing T -linear resistivity, *Science* **339**, 804 (2013).
- [18] C. M. Varma, Colloquium: Linear in temperature resistivity and associated mysteries including high temperature superconductivity, *Rev. Mod. Phys.* **92**, 031001 (2020).
- [19] D. V. Else and T. Senthil, Strange Metals as Ersatz Fermi Liquids, *Phys. Rev. Lett.* **127**, 086601 (2021).
- [20] H. Takagi, B. Batlogg, H. L. Kao, J. Kwo, R. J. Cava, J. J. Krajewski, and W. F. Peck, Systematic Evolution of Temperature-Dependent Resistivity in $\text{La}_{2-x}\text{Sr}_x\text{CuO}_4$, *Phys. Rev. Lett.* **69**, 2975 (1992).
- [21] Y. Nam, D. K. Ki, D. Soler-Delgado, and A. F. Morpurgo, Electron-hole collision limited transport in charge-neutral bilayer graphene, *Nat. Phys.* **13**, 1207 (2017).
- [22] G. R. Stewart, Non-Fermi-liquid behavior in d - and f -electron metals, *Rev. Mod. Phys.* **73**, 797 (2001).
- [23] L. Balents and M. P. A. Fisher, Correlation effects in carbon nanotubes, *Phys. Rev. B* **55**, R11973 (1997).
- [24] B. Bertini, F. Heidrich-Meisner, C. Karrasch, T. Prosen, R. Steinigeweg, and M. Žnidarič, Finite-temperature transport in one-dimensional quantum lattice models, *Rev. Mod. Phys.* **93**, 025003 (2021).
- [25] K. V. Samokhin, Lifetime of excitations in a clean Luttinger liquid, *J. Phys.: Condens. Matter* **10**, L533 (1998).
- [26] K. A. Matveev and A. Furusaki, Decay of Fermionic Quasiparticles in One-Dimensional Quantum Liquids, *Phys. Rev. Lett.* **111**, 256401 (2013).
- [27] Y. Huang, C. Karrasch, and J. E. Moore, Scaling of electrical and thermal conductivities in an almost integrable chain, *Phys. Rev. B* **88**, 115126 (2013).
- [28] V. B. Bulchandani, C. Karrasch, and J. E. Moore, Superdiffusive transport of energy in one-dimensional metals, *Proc. Natl. Acad. Sci. USA* **117**, 12713 (2020).
- [29] K. Damle and S. Sachdev, Nonzero-temperature transport near quantum critical points, *Phys. Rev. B* **56**, 8714 (1997).
- [30] S. Sachdev, Theory of finite-temperature crossovers near quantum critical points close to, or above, their upper-critical dimension, *Phys. Rev. B* **55**, 142 (1997).
- [31] S. Sachdev, Nonzero-temperature transport near fractional quantum Hall critical points, *Phys. Rev. B* **57**, 7157 (1998).
- [32] L. D. Landau and E. M. Lifshitz, *Fluid Mechanics*, Course of Theoretical Physics Vol. 6 (Elsevier, Amsterdam, 2013).
- [33] L. P. Kadanoff and P. C. Martin, Hydrodynamic equations and correlation functions, *Ann. Phys.* **24**, 419 (1963).
- [34] M. Dupont and J. E. Moore, Universal spin dynamics in infinite-temperature one-dimensional quantum magnets, *Phys. Rev. B* **101**, 121106(R) (2020).
- [35] S. R. White, Density Matrix Formulation for Quantum Renormalization Groups, *Phys. Rev. Lett.* **69**, 2863 (1992).
- [36] G. Vidal, Efficient Classical Simulation of Slightly Entangled Quantum Computations, *Phys. Rev. Lett.* **91**, 147902 (2003).
- [37] G. Vidal, Classical Simulation of Infinite-Size Quantum Lattice Systems in One Spatial Dimension, *Phys. Rev. Lett.* **98**, 070201 (2007).

- [38] U. Schollwöck, The density-matrix renormalization group in the age of matrix product states, *Ann. Phys.* **326**, 96 (2011).
- [39] Since there are different terminologies appearing in the literature, note that particle-hole scattering can also be viewed as a kind of two-particle umklapp scattering but with no loss of momentum, as explained below Fig. 1.
- [40] C. Xu and J. E. Moore, Stability of the quantum spin Hall effect: Effects of interactions, disorder, and \mathbb{Z}_2 topology, *Phys. Rev. B* **73**, 045322 (2006).
- [41] C. Wu, B. A. Bernevig, and S. C. Zhang, Helical Liquid and the Edge of Quantum Spin Hall Systems, *Phys. Rev. Lett.* **96**, 106401 (2006).
- [42] E. Fradkin, *Field Theories of Condensed Matter Physics* (Cambridge University Press, Cambridge, UK, 2013).
- [43] R. Shankar, *Quantum Field Theory and Condensed Matter: An Introduction* (Cambridge University Press, Cambridge, U.K., 2017).
- [44] See Supplemental Material at <http://link.aps.org/supplemental/10.1103/PhysRevB.107.L100301>, which provides a general review for the motivation, details for fast umklapp scattering, pedagogical calculations via kinetic theory, transformation from fermion model to spin model and the breaking of integrability, as well as the DMRG details.
- [45] P. Arnold, G. D. Moore, and L. G. Yaffe, Transport coefficients in high temperature gauge theories (I): Leading-log results, *J. High Energy Phys.* **11** (2000) 001.
- [46] Note that we only have two integrals and one delta function on the right-hand side of Eq. (10), as the conservation of energy and conservation of momentum have the same requirement for linear dispersion in one dimension.
- [47] This is in accordance with the fact that the 1D chiral fluid cannot be relaxed in the absence of impurities (see Supplemental Material [44]).
- [48] T. Giamarchi, *Quantum Physics in One Dimension* (Oxford University Press, Oxford, UK, 2004).
- [49] J. Sirker, R. G. Pereira, and I. Affleck, Diffusion and Ballistic Transport in One-Dimensional Quantum Systems, *Phys. Rev. Lett.* **103**, 216602 (2009).
- [50] M. S. Bahovadinov, O. Gülseren, and J. Schnack, Local entanglement and string order parameter in dimerized models, *J. Phys.: Condens. Matter* **31**, 505602 (2019).
- [51] H. Bruus and J. C. Anglès d'Auriac, Energy level statistics of the two-dimensional Hubbard model at low filling, *Phys. Rev. B* **55**, 9142 (1997).
- [52] R. Kubo, Statistical-mechanical theory of irreversible processes. I. General theory and simple applications to magnetic and conduction problems, *J. Phys. Soc. Jpn.* **12**, 570 (1957).
- [53] R. Kubo, M. Yokota, and S. Nakajima, Statistical-mechanical theory of irreversible processes. II. Response to thermal disturbance, *J. Phys. Soc. Jpn.* **12**, 1203 (1957).
- [54] J. M. Luttinger, Theory of thermal transport coefficients, *Phys. Rev.* **135**, A1505 (1964).
- [55] A. Kapustin and L. Spodyneiko, Absence of Energy Currents in an Equilibrium State and Chiral Anomalies, *Phys. Rev. Lett.* **123**, 060601 (2019).
- [56] A. E. Feiguin and S. R. White, Finite-temperature density matrix renormalization using an enlarged Hilbert space, *Phys. Rev. B* **72**, 220401(R) (2005).
- [57] C. Karrasch, J. H. Bardarson, and J. E. Moore, Reducing the numerical effort of finite-temperature density matrix renormalization group calculations, *New J. Phys.* **15**, 083031 (2013).
- [58] T. Barthel, Matrix product purifications for canonical ensembles and quantum number distributions, *Phys. Rev. B* **94**, 115157 (2016).
- [59] J. Haegeman, C. Lubich, I. Oseledets, B. Vandereycken, and F. Verstraete, Unifying time evolution and optimization with matrix product states, *Phys. Rev. B* **94**, 165116 (2016).
- [60] C. Hubig, I. P. McCulloch, and U. Schollwöck, Generic construction of efficient matrix product operators, *Phys. Rev. B* **95**, 035129 (2017).
- [61] D. M. Kennes and C. Karrasch, Extending the range of real time density matrix renormalization group simulations, *Comput. Phys. Commun.* **200**, 37 (2016).
- [62] H. Yoshioka and A. A. Odintsov, Electronic Properties of Armchair Carbon Nanotubes: Bosonization Approach, *Phys. Rev. Lett.* **82**, 374 (1999).
- [63] T. M. Rice, N. J. Robinson, and A. M. Tsvelik, Umklapp scattering as the origin of T -linear resistivity in the normal state of high- T_c cuprate superconductors, *Phys. Rev. B* **96**, 220502(R) (2017).
- [64] S. Sachdev and J. Ye, Gapless Spin-Fluid Ground State in a Random Quantum Heisenberg Magnet, *Phys. Rev. Lett.* **70**, 3339 (1993).
- [65] E. H. Lieb and W. Liniger, Exact analysis of an interacting Bose gas. I. The general solution and the ground state, *Phys. Rev.* **130**, 1605 (1963).
- [66] S. Hild, T. Fukuhara, P. Schauß, J. Zeiher, M. Knap, E. Demler, I. Bloch, and C. Gross, Far-from-Equilibrium Spin Transport in Heisenberg Quantum Magnets, *Phys. Rev. Lett.* **113**, 147205 (2014).
- [67] Y. Tang, W. Kao, K. Y. Li, S. Seo, K. Mallayya, M. Rigol, S. Gopalakrishnan, and B. L. Lev, Thermalization Near Integrability in a Dipolar Quantum Newton's Cradle, *Phys. Rev. X* **8**, 021030 (2018).
- [68] E. W. Huang, R. Sheppard, B. Moritz, and T. P. Devereaux, Strange metallicity in the doped Hubbard model, *Science* **366**, 987 (2019).